13

Focusing of converging hypersonic frequency surface acoustic waves on NiCu/diamond structure

© A.Yu. Klokov, N.Yu. Frolov, A.I. Sharkov, S.I. Chentsov

Lebedev Physical Institute, Russian Academy of Sciences, Moscow, Russia
E-mail: klokov@lebedev.ru

Received April 17, 2025
Revised June 17, 2025
Accepted August 3, 2025

The propagation of converging surface acoustic waves on the surface of a natural diamond plate with the orientation (001), generated by ring optical excitation, is experimentally studied. It is shown that, despite the elastic anisotropy of diamond and the presence of dispersion, the surface wave field at the focus can be concentrated into a spot with dimensions less than $\sim 4\,\mu$m, which is close to the diffraction limit. The wave magnitude at the focal point is 15 times greater than the wave magnitude in the excitation region. The results obtained create prerequisites for the implementation of ultra-high dynamic deformations at the focal point of the converging surface wave, which radically reduce the requirements for the radiation resistance of the material.

Keywords: surface acoustic waves, converging surface waves, diamond, hypersound.

DOI: 10.61011/TPL.2025.11.62202.20346

Methods of local (targeted) processing of natural and synthetic diamonds, which make it possible to control the properties of color centers contained in them, have been advancing rapidly in recent years [1–6]. Potential applications of such methods include the design of various photooptical, photothermal, and photovoltaic devices [1–6]. The overwhelming majority of these methods rely on the effect of pulsed laser irradiation, which induces a rearrangement of impurities and defects in the exposed region [1–3]. The effect is multifactorial and difficult to control, since the local restructuring of centers is accompanied by nonequilibrium relaxation of the electronic subsystem. An alternative solution, which is not associated with excitation of the electronic subsystem, is to expose the diamond matrix and color centers located in it to high-amplitude elastic waves [4].

However, even with an optimum set of irradiation parameters, restrictions tied to radiation resistance limit the maximum dynamic deformation in standard experiments with laser-induced generation of hypersonic waves with a diverging or planar front in the thermoelastic regime to $10^{-5}-10^{-3}$ (see theoretical study [7] and references therein), which is insufficient for rearrangement of the crystalline structure of a material or defects in it. The present study is the first to demonstrate the possibility of generation of converging surface acoustic waves (SAWs) of hypersonic frequencies propagating along the surface of diamond. A ring laser excitation arrangement, where the power density of radiation is more than three orders of magnitude lower than the one in standard experiments on excitation of diverging hypersonic waves, was used to excite converging waves. It was found that, despite the presence of dispersion and anisotropy of the group velocity, converging waves may be focused into a region several micrometers in size with large-amplitude dynamic deformation. The used technique for generating converging pulses of hypersonic surface waves is of interest for expanding the arsenal of methods for controlled manipulation of color centers in diamonds.

The sample under study was a natural type Ia diamond wafer with a thickness of $\sim 180\,\mu$m and the (001) orientation. A thin NiCu film 60 nm in thickness was deposited onto its surface [8]. A setup implementing the two-color „pump–probe“ technique was used to generate and record SAW pulses. A femtosecond Ti:Sa Mira-900 laser (pulse duration, 170 fs; repetition rate, 76 MHz; wavelength, 800 nm) served as a radiation source. This radiation was split into two beams. Following frequency doubling, the second beam (wavelength, 400 nm; pulse energy, < 1 nJ) was absorbed in the metal film. The thermoelastic effect in the NiCu/diamond structure induced a bulk elastic pulse propagating into the depth of the sample and a surface acoustic wave.

The propagating SAW pulse changed the phase of the complex reflection coefficient by as much as $\sim 10^{-3}$ rad. These variations were identified by monitoring the reflection of a probing laser pulse (energy, 0.05 nJ) at the radiation source wavelength with a modified Sagnac interferometer [9]. A 4f scanner was introduced into the setup in order to scan the surface with the probing beam. An optical delay line in the recording channel provided an opportunity to observe the spatial elastic field pattern at different moments in time relative to the excitation pulse.

To generate a converging SAW pulse, an axicon with an angle of 1.0° and a lens with an aperture of 0.65 could be introduced into the excitation channel. With this configuration of the setup, a ring-shaped distribution of light intensity with an approximate diameter of $60\,\mu$m and a width of $2-3\,\mu$m was formed on the sample surface. In

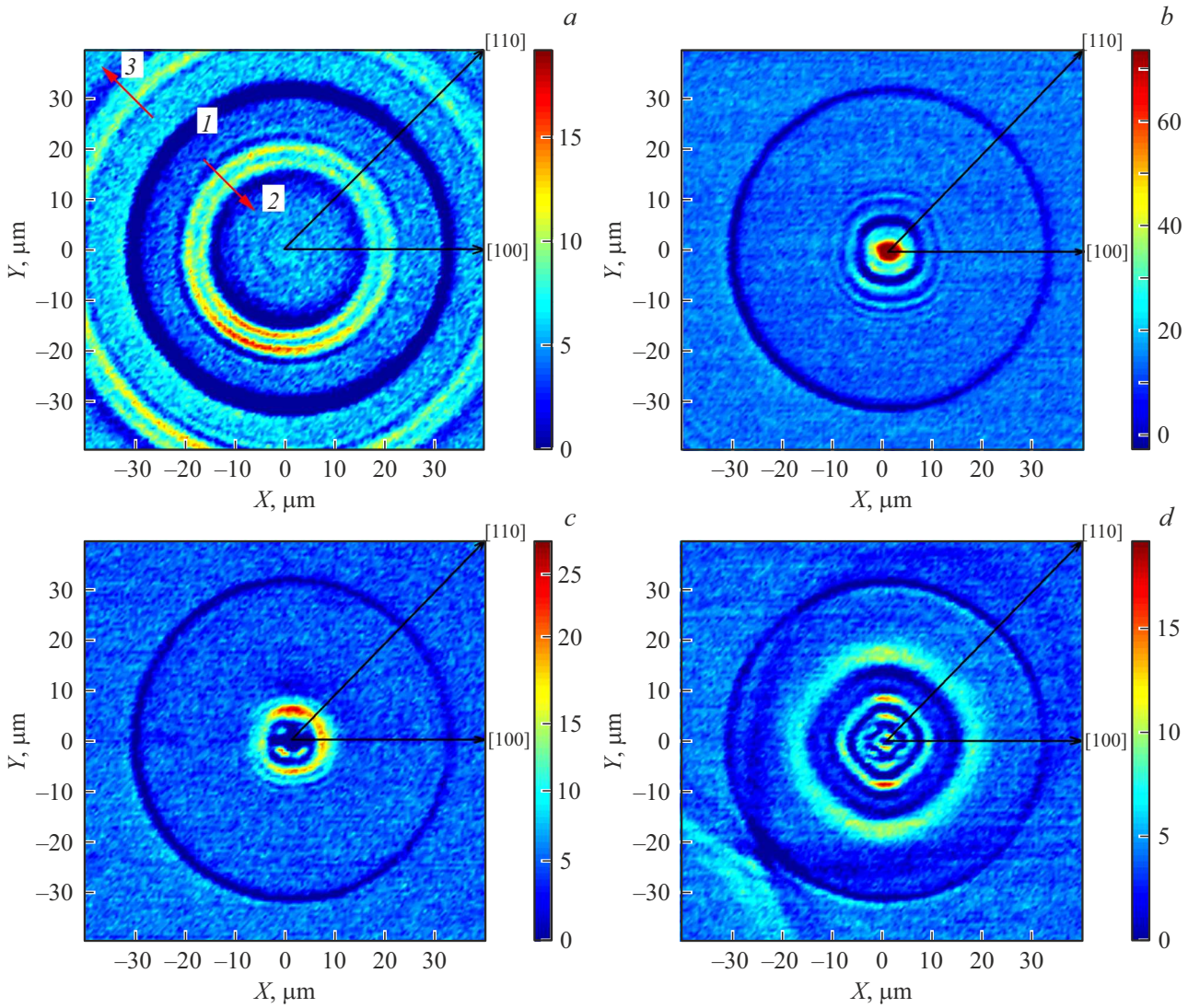

Figure 1. SAW pulse field at the following moments in time: 1616 (a), 3056 (b), 3556 (c), and 4556 ps (d). The color scale represents the surface displacement in picometers (except for the annular excitation region). In panel a, dark ring *1* is the excitation region and arrows *2* and *3* indicate the direction of propagation of a SAW pulse. A color version of the figure is provided in the online version of the paper.

this case, Rayleigh-type SAW pulses with a wavelength on the order of the ring width (the spectral width was on the order of 4 GHz, and the spectrum maximum was at ~ 3 GHz) were generated, and the penetration depth was $4-5\,\mu$m. This implies that a SAW pulse is localized largely in diamond, and the NiCu film plays a secondary role, although it does induce dispersion. The estimated group velocity of a Rayleigh SAW in our experiment varies within $\sim 20\,\%$. Higher modes (e.g., the Sezawa wave) are not excited, since the wave vectors are limited from above by the value of $2\pi/d \approx 2\,\text{rad}/\mu\text{m}$ (d is the width of the excitation ring), which is lower than the calculated critical value of $\sim 5\,\text{rad}/\mu\text{m}$. The energy exposure was $\sim 7\,\mu\text{J/cm}^2$, which is ~ 400 times lower than the optical damage threshold of the sample. The setup was discussed in detail in [10].

Figures 1, $a-d$ present the converging SAW pulse patterns at different moments of time under ring optical excitation, while Figs. 2, $a-d$ show the SAW pulse profiles recorded the same moments of time as in Figs. 1, $a-d$, respectively, along the lines passing through the focal point of the SAW pulse, which are equivalent to $\{100\}$ and $\{110\}$.

Since heating of the sample surface also leads to a change in phase of the reflection coefficient due to the thermo-optic effect, the region heated by a laser pulse is represented by a dark ring (*1* in Fig. 1, a) in all figures. The radius of the ring is $32\,\mu$m, which is less than the distance of SAW travel in one laser pulse repetition period ($\sim 140\,\mu$m); therefore, the waves excited by an earlier pulse diverge by the time the next excitation pulse arrives (see also Fig. 2, a). Figure 1, a, which corresponds to a delay of 1616 ps, reveals that two Rayleigh SAW fronts

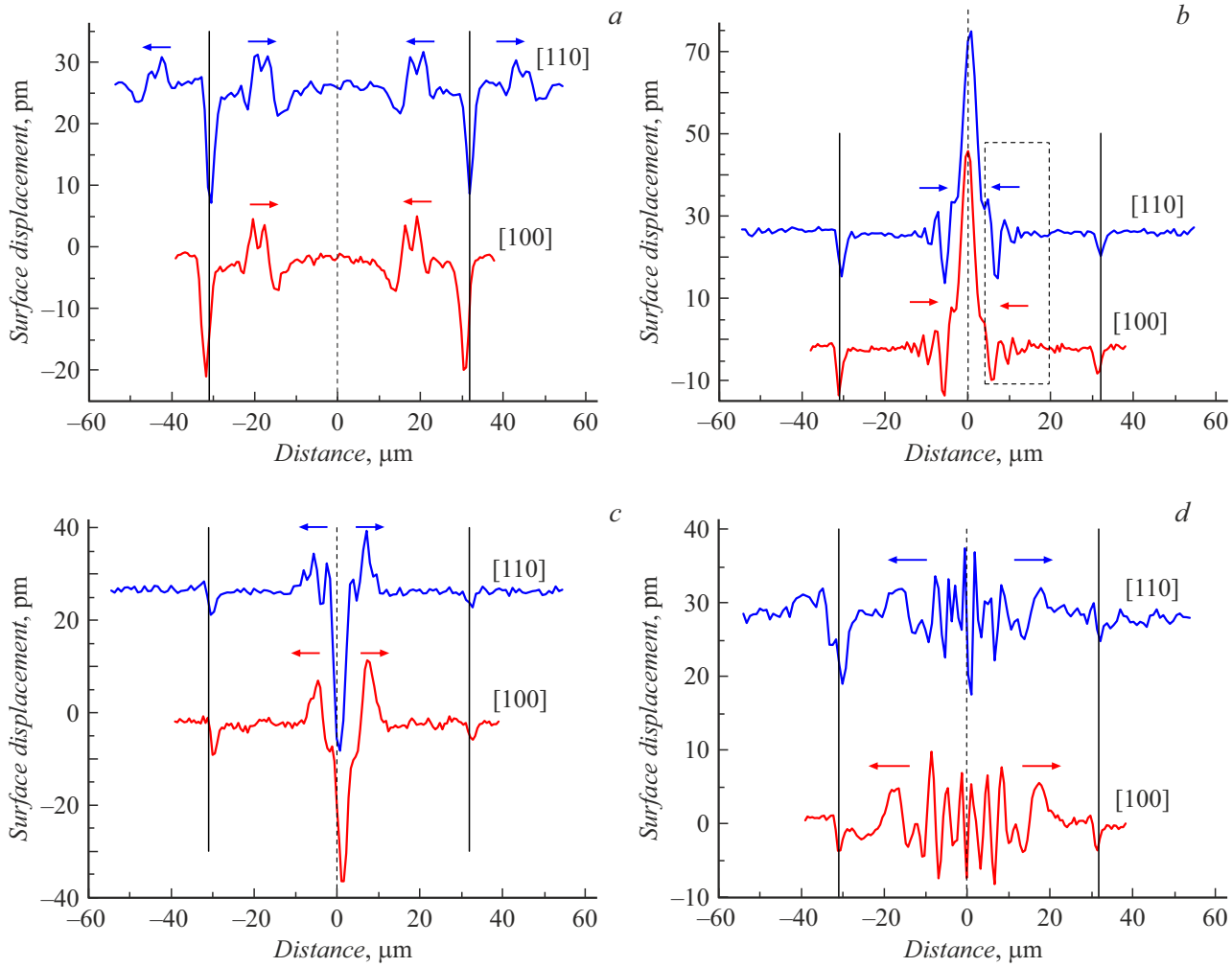

Figure 2. SAW pulse profiles at 1616 (*a*), 3056 (*b*), 3556 (*c*), and 4556 ps (*d*) recorded along the directions equivalent to {100} and {110} shown in Fig. 1. Thin solid vertical lines denote the excitation region, and the dotted vertical line is the approximate focal point. Arrows indicate the direction of propagation of a SAW pulse. Color online.

diverge from the excitation region into the excitation ring (indicated by the arrow with number *2*) and away from it (indicated by the arrow with number *3*). Since the SAW pulse velocity at the (001) diamond cut depends only weakly on the direction of propagation and the distance traveled is small ($\sim 18\,\mu$m), the shape of fronts differs little from a ring. Figure 2, *a* provides an opportunity to estimate the propagation velocity of converging SAW pulses, which was found to be $\sim 10.8\,\mu$m/ns. The propagation velocity anisotropy starts to manifest itself in Fig. 1, *b*, which corresponds to a delay of 3056 ps (the moment of SAW pulse focusing; i. e., the leading front „collapse"). The fronts have the form of a rounded square, which is characteristic of fourth-order symmetry and corresponds to a diamond wafer with the (001) orientation. In addition, several successive fronts, which are induced by the frequency dispersion of SAW pulses arising due to loading of the diamond surface by the NiCu film, are seen. Examining the area highlighted by the dotted rectangle in Fig. 2, *b*, one can see that higher-frequency components of SAW pulses lag noticeably behind the relatively low-frequency ones forming the leading front. However, the profiles shown in Fig. 2, *b* (3056 ps, which is the maximum focusing time) make it clear that the major part of the SAW pulse energy in all directions is focused into a spot $\sim 4\,\mu$m in size (FWHM), which is close to the excitation ring width ($3\,\mu$m) and to the SAW pulse wavelength corresponding to the spectrum maximum ($\sim 3.6\,\mu$m).

Figure 1, *c*, which corresponds to a delay of 3556 ps, presents the field pattern after the passage of a SAW pulse through the focus, which is accompanied by a change in polarity of the response (Fig. 2, *c*). With further propagation (Fig. 1, *d*, 4556 ps), the wave front also assumes the shape of a rounded square, but it is „rotated" by 45° relative to the front pattern before focusing. This „rotation" may be attributed to the fact that waves propagating in a „faster" direction (i. e., {001}) pass the focal point earlier and move away from it.

A comparison of the profiles of the converging SAW pulse in Figs. 2, *a* and *b* reveals a 12-fold increase in magnitude

of the response (and a 15-fold growth in comparison with the magnitude in the excitation region), which implies a corresponding increase in deformation of the sample material. The estimated deformation at the focus is $2 \cdot 10^{-5}$. The pulse duration at the focus may be estimated by the time it takes for an elastic pulse to pass through the focal region, which is ~ 400 ps. In the present study, we are limited in generation by the maximum laser pulse energy. Nevertheless, as was noted above, we have a ~ 400-fold radiation resistance margin. Therefore, deformations at the level of $8 \cdot 10^{-3}$ are expected to be achievable in the discussed geometry. This value may be increased through the use of a larger ring for SAW pulse excitation. In addition, as was demonstrated in [10], it is possible to adjust the distribution and structure of the SAW pulse field at the focus by altering the shape of the excitation region (e. g., by shading a part of the ring). This feature may be of interest in studies of the local morphology and/or electronic properties of various defect systems.

Thus, the excitation and propagation of converging SAW pulses on the surface of diamond with the (001) orientation were investigated. It was found that a SAW pulse is focused into a spot $\sim 4\,\mu$m in size, which is close to the diffraction limit. It was demonstrated that the use of ring optical excitation allows one to relax the requirements as to radiation resistance of the sample, which is crucial for achieving extreme levels of deformation (10^{-2}) up to acoustic breakdown that is accompanied by modification of the material.

Acknowledgments

The authors wish to thank S.A. Evlashin and R.A. Khmel'nitskii for providing diamond samples with NiCu films and S.N. Nikolaev for fruitful discussions.

Funding

This study was supported by the Russian Science Foundation (project No. 24-72-00132).

Conflict of interest

The authors declare that they have no conflict of interest.

References

[1] Z. Ju, J. Lin, S. Shen, B. Wu, E. Wu, Adv. Phys. X, **6** (1), 1858721 (2021). DOI: 10.1080/23746149.2020.1858721
[2] X. Wang, H. Fang, F. Sun, H. Sun, Laser Photon. Rev., **16** (1), 2100029 (2021). DOI: 10.1002/lpor.202100029
[3] S.I. Kudryashov, V.G. Vins, P.A. Danilov, E.V. Kuzmin, A.V. Muratov, G.Yu. Kriulina, J. Chen, A.N. Kirichenko, Y.S. Gulina, S.A. Ostrikov, P.P. Paholchuk, M.S. Kovalev, N.B. Rodionov, A.O. Levchenko, Carbon, **201**, 399 (2023). DOI: 10.1016/j.carbon.2022.09.040
[4] D.A. Golter, T. Oo, M. Amezcua, I. Lekavicius, K.A. Stewart, H. Wang, Phys. Rev. X, **6**, 041060 (2016). DOI: 10.1103/PhysRevX.6.041060
[5] A.M. Gorbachev, M.A. Lobaev, D.B. Radishchev, A.L. Vikharev, S.A. Bogdanov, S.V. Bol'shedvorskii, A.I. Zeleneev, V.V. Soshenko, A.V. Akimov, M.N. Drozdov, V.A. Isaev, Tech. Phys. Lett., **46** (7), 641 (2020). DOI: 10.1134/S063785020070093.
[6] R.A. Babunts, A.S. Gurin, A.P. Bundakova, M.V. Muzafarova, A.N. Anisimov, P.G. Baranov, Tech. Phys. Lett., **49** (1), 40 (2023). DOI: 10.21883/TPL.2023.01.55346.19391.
[7] M.V. Shugaev, L.V. Zhigilei, J. Appl. Phys., **130**, 185108 (2021). DOI: 10.1063/5.0071170
[8] S.A. Evlashin, V.P. Martovitskii, R.A. Khmel'nitskii, A.S. Stepanov, N.V. Suetin, P.V. Pashchenko, Tech. Phys. Lett., **38** (5), 418 (2012). DOI: 10.1134/S1063785012050057.
[9] T. Tachizaki, T. Muroya, O. Matsuda, Y. Sugawara, D. Hurley, O. Wright, Rev. Sci. Instrum., **77**, 043713 (2006). DOI: 10.1063/1.2194518
[10] A.Yu. Klokov, V.S. Krivobok, A.I. Sharkov, N.Yu. Frolov, Sensors, **22**, 870 (2022). DOI: 10.3390/s22030870

Translated by D.Safin